IOP Conf. Series: Journal of Physics: Conf. Series **875** (2017) 012013 doi:10.1088/1742-6596/875/2/012013

Lifetimes of ultralong-range strontium Rydberg molecules in cold dense gases

J. D. Whalen, F. Camargo, R. Ding, T. C. Killian, F. B. Dunning

E-mail: fbd@rice.edu
Department of Physics and Astronomy, Rice University, Houston, TX 77005, USA

J. Pérez-Ríos

Department of Physics and Astronomy, Purdue University, West Lafayette, IN 47907, USA, and School of Material Sciences and Technology, Universidad del Turabo, Gurabo, PR 00778, USA

S. Yoshida, J. Burgdörfer

Institute for Theoretical Physics, Vienna University of Technology, Vienna, Austria, EU

Abstract. The lifetimes and decay channels of ultralong-range Rydberg molecules created in a dense Bose-Einstein condensate (BEC) are examined by monitoring the time evolution of the Rydberg population using field ionization. The Rydberg molecules, which contain tens to hundreds of ground state atoms within the electron orbit, have lifetimes of ~ 1 to 5 μs, their destruction being attributed to two main processes: formation of Sr_2^+ ions through associative ionization, and dissociation induced through L-changing reactions. The observed loss rates are consistent with a reaction model that emphasizes the interaction between the Rydberg core ion and its nearest neighbor ground state atom. The application of this model to earlier measurements of strontium dimer lifetimes at lower densities is discussed.

Much interest has been focused on the physical and chemical properties of ultralong-range Rydberg molecules which comprise a Rydberg atom bound to one, or more, ground-state atoms through scattering of the Rydberg electron. The existence of such species was first predicted theoretically [1]. The interaction between the Rydberg electron and ground state atom(s) was described by a Fermi pseudopotential and results in a molecular potential that can bind multiple vibrational levels. Initial experiments, in a cold thermal gas, centered on rubidium dimer molecules [2]. Measurements of dimer molecules have now been extended to other atomic species including strontium and cesium, to anisotropic p and d Rydberg states, and (using Cs(ns) Rydberg states) to creation of so-called trilobite molecules which, although homonuclear, possess large permanent electric dipole moments [3–12]. Detailed spectroscopic studies have demonstrated the formation of molecules containing four or more ground state atoms [13]. Measurements in rubidium have been extended to BECs with peak densities approaching 10^{15} cm^{-3}, sufficient that, for values of $n \gtrsim 50$, the Rydberg electron orbit can enclose tens to hundreds of ground-state atoms [14, 15].

Recent work suggests that Rydberg molecules might be used to probe the properties of cold dense gases including examining collective phenomena such as the creation of polarons

in quantum degenerate gases [16] and imaging the Rydberg electron wave function [17–19]. However, the use of Rydberg molecules in such applications requires that their lifetimes be sufficient to allow their interactions time to produce measurable effects. This has stimulated interest in the study of Rydberg molecule lifetimes and in the mechanisms responsible for their destruction.

Initial studies of Rydberg molecule lifetimes used cold thermal gases and centered on Rb($35s$)-Rb dimers [15]. These measurements showed that the lifetime of the dimer molecules was significantly less than that of the parent $35s$ atoms and that their lifetimes decreased with increasing vibrational excitation, behavior that was attributed to the presence of a strong p-wave shape resonance in low-energy electron scattering from rubidium. A sizable increase in the molecular loss rate was seen with increasing density in the trap, the cross section for loss being comparable to the geometric size of the molecule. Studies of molecular lifetimes in a rubidium BEC also revealed sizable collisional loss rates, $\sim 10^5$ to 10^6 s^{-1}, that were attributed to formation of Rb_2^+ ions through associative ionization and to L-changing reactions involving the Rydberg electron [20].

Strontium has no low-energy p-wave scattering resonance and studies of strontium dimers in cold thermal gases revealed behavior rather different from that seen in rubidium [21]. The lifetimes of low-lying dimer states were found to be very similar to that of the parent atomic Rydberg state and less sensitive to the atom density in the trap pointing to a small cross section for collisional loss. Here we explore the lifetimes of Rydberg molecules with n=49, 60, and 72 created in a strontium BEC having a peak density of $\sim 4\times10^{14}$ cm^{-3}. As in the earlier rubidium studies, sizable loss rates, $\sim 5 \times 10^5$ s^{-1}, are observed. The observations are consistent with the predictions of a classical model of the reaction dynamics which emphasizes the role of the interaction between the Rydberg core ion and the nearest ground-state atom. The application of this model to the earlier dimer measurements is discussed.

The techniques used to cool and trap strontium atoms are described in detail elsewhere [22]. Briefly, ^{84}Sr atoms are initially cooled in a "blue" magneto-optical trap (MOT) operating on the $5s^2\ ^1S_0 - 5s5p\ ^1P_1$ transition at 461 nm whereupon the atom temperature is further reduced using a "red" MOT utilizing the $5s^2\ ^1S_0 - 5s5p\ ^3P_1$ intercombination line at 689 nm. The atoms are then loaded into an optical dipole trap (ODT) formed by two crossed 1.06 μm laser beams with $\sim$60 μm waists where they are subject to evaporative cooling to create a BEC. The trap density was determined from measurements of the total atom number and trap oscillation frequencies. Typically $\sim 4 \times 10^5$ atoms are trapped with a peak density of $\sim 4 \times 10^{14}$ cm^{-3} for which density molecules with $n = 49(72)$ contain $\sim 15(170)$ ground state atoms within the electron cloud.

Rydberg atoms/molecules are excited to the $5sns\ ^3S_1$ state by two-photon excitation via the intermediate $5s5p\ ^3P_1$ level using radiation at 689 and 319 nm. The 689 nm laser for the first step is tuned 80 MHz to the blue of the intermediate state to avoid scattering. The 319 nm laser is tuned to the atomic or molecular state of interest. The number of Rydberg atoms/molecules present in the ODT is determined by selective field ionization (SFI). An electric field ramp is applied and the number of electrons liberated is determined as a function of time during the ramp using a microchannel plate whose output pulses are fed to a multichannel scaler (MCS). The field at which ionization occurs is determined from the electron arrival time at the MCP.

To measure lifetimes/decay rates the apparatus is operated in a pulsed mode. The excitation lasers are chopped to form a periodic train of optical pulses with a pulse repetition frequency of $\sim$ 4 kHz and pulse duration of $\sim$ 2 μs. The ODT is turned off during excitation to eliminate AC Stark shifts. Following excitation, the number of surviving Rydberg atoms/molecules is measured as a function of time delay, t_D, using SFI.

Figure 1 shows the time evolution of the total SFI signal following creation of $n = 60$ Rydberg molecules at detunings of -13.6 and -21.6 MHz. Similar time evolutions are seen for $n = 49$

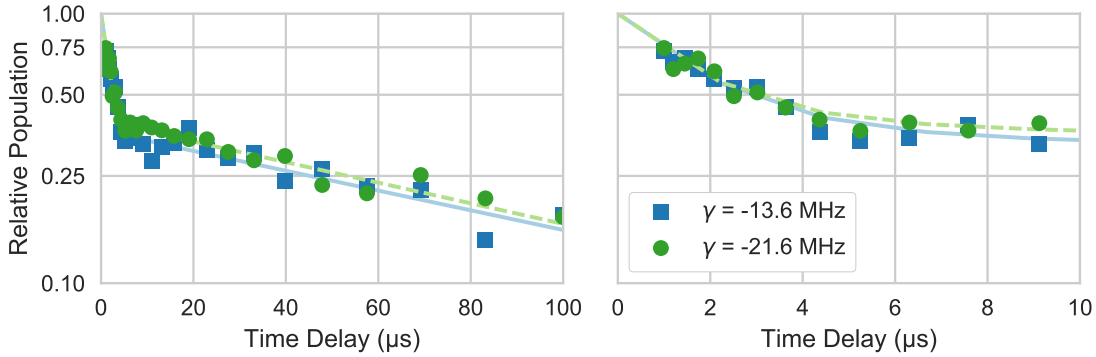

Figure 1. Left: Time dependence of the total SFI signal for $n = 60$ Rydberg molecules and the detunings, γ, indicated. Both data sets are normalized to one at $t_D = 0$. The solid and dashed lines are fits to the data obtained using Eqs. 6 (see text) for detunings of -13.6 MHz and -21.6 MHz respectively. Right: Expanded view at short time delays.

and $n = 72$ molecules. Large detunings are selected as they correspond to the largest numbers of ground state atoms within the electron cloud, i.e., the largest local atom density, ρ. For large atom densities the detuning, ΔE, and ρ are approximately related by the mean-field expression

$$\Delta E = \frac{2\pi\hbar^2}{m_e} A_s(k)\rho \tag{1}$$

where m_e is the electron mass and $A_s(k)$ is the momentum-dependent s-wave scattering length. As seen in Fig. 1, the SFI signal initially decreases rapidly with increasing time delay. The rate of decrease slows and becomes constant at later times. This behavior can be explained by considering the processes that can lead to destruction of a Rydberg molecule. These include associative ionization

$$\mathrm{Sr}^M(n^3\mathrm{S}_1) + \mathrm{Sr} \rightarrow \mathrm{Sr}_2^+ + \mathrm{e}^- \tag{2}$$

where Sr^M denotes a Rydberg atom forming the core of a molecule; L-changing reactions

$$\mathrm{Sr}^M(n^3\mathrm{S}_1) + \mathrm{Sr} \rightarrow \mathrm{Sr}(n'L') + \mathrm{Sr} \tag{3}$$

in which the Rydberg electron transitions to a nearby lower-lying Rydberg state (typically, for strontium, $(n\text{-}4)L$ states with $L \geq 4$) [20]; and radiative processes, i.e., spontaneous emission or interactions with background blackbody radiation. As will be shown, reactions (2) and (3) are responsible for the bulk of the present Rydberg molecule loss. Reaction (2) requires a close collision between the Rydberg core ion and a ground state atom together with the presence of the Rydberg electron to carry off the molecular binding energy. Considerations of momentum conservation require that L-changing also involve a similar close collision. The energy released, $\sim 1/n^3$ a.u. ($\sim$30 GHz at $n = 60$), is sufficient to give the core ion and ground-state atom velocities of $\sim 10\ \mathrm{m\,s^{-1}}$. The excited electron remains bound to the core ion producing a fast Rydberg atom that escapes the ODT on a time scale of $\sim 1\ \mu$s after which it undergoes no further collisions. However, these Rydberg atoms remain within 1 to 2 mm of the ODT over the duration of the present experiments and thus contribute to the total SFI signal. (SFI spectra seen at late times differ markedly from those seen at early times, the changes being consistent with population of higher-L states with values of n close to that of the parent molecules.)

The experimental results can be fitted using a simple rate equation model which assumes that Rydberg molecules are lost through reactions (2) and (3), with rates Γ_{AI} and Γ_L, respectively,

and radiative processes with rate Γ_R. Given that the measurements show the radiative decay rates of the L-changed atoms are similar to those of the parent Rydberg atoms and, by extension, the parent molecules, the time evolution of the populations N_P and N_L of parent Rydberg molecules and L-changed atoms can be written

$$\frac{\mathrm{d}N_P}{\mathrm{d}t} = -(\Gamma_{AI} + \Gamma_L + \Gamma_R)N_P. \tag{4}$$

$$\frac{\mathrm{d}N_L}{\mathrm{d}t} = \Gamma_L N_P - \Gamma_R N_L \tag{5}$$

Analytic solution of these equations yields

$$\begin{aligned} N_P &= N_0 e^{-(\Gamma_{AI}+\Gamma_L+\Gamma_R)t} \\ N_L &= N_0 \frac{\Gamma_L}{\Gamma_{AI}+\Gamma_L} e^{-\Gamma_R t}\left[1 - e^{-(\Gamma_{AI}+\Gamma_L)t}\right] \end{aligned} \tag{6}$$

Analysis of the late time data, where N_P is very small, is first used to obtain the radiative decay rate Γ_R, $\sim 10^4$ s^{-1}, a value very similar to that of the parent atoms. The measured sum, $N_P + N_L$, is then fitted using Eqs. 6 by adjusting the parameters N_0, Γ_{AI}, and Γ_L. The resulting best fits are included in Fig. 1 and the corresponding total molecular destruction rates, $\Gamma_{LOSS} = \Gamma_{AI} + \Gamma_L$, are shown in Fig. 2 as a function of local atom density, ρ. Figure 2 also includes results obtained using $n = 49$ and $n = 72$ molecules. For each value of n the rates Γ_{AI} and Γ_L were equal to within $\pm 20\%$. Although large, the measured destruction rates are similar to those seen in the earlier rubidium studies for the same range of n [20].

The experimental observations are consistent with the predictions of a model which recognizes that, because of the very low temperature of the BEC (~ 150 nK), any initial relative motions of the Rydberg core ion and neighboring ground-state atoms must be very small. Reaction is therefore presumed to be initiated by the mutual attraction between the Rydberg core ion and nearest ground-state atom. Monte Carlo sampling of initial conditions is used to estimate the time required for these to collide, their mutual attraction being described by a C_4/r^4 potential. Since, at high local densities, the separation between the core ion and nearest ground-state atom is much smaller than the radius of the Rydberg electron orbit, electron screening of the core ion field should be small and is neglected. In the simulations 1000 ground state atoms are uniformly distributed in a box with the Sr^+ core ion at the center (the size of the box is changed to vary the density). The closest neutral atom to the Sr^+ ion core is then selected and the time they take to collide computed using

$$t = \int_{r_{\mathrm{intial}}}^{r_{\mathrm{final}}} \frac{\mathrm{d}r}{v(r)} = \int_{r_{\mathrm{intial}}}^{r_{\mathrm{final}}} \frac{\mathrm{d}r}{\sqrt{\frac{2}{\mu}\left(E_{\mathrm{coll}} + \frac{C_4}{r^4}\right)}}\,, \tag{7}$$

where r_{intial} and $r_{\mathrm{final}}(=0)$ are the initial and final inter-particle separations, μ is the reduced mass, and E_{coll} is the initial collision energy. Upon collision, reaction, either associative ionization or L-changing, is presumed to occur. The calculations are repeated for many initial ground-state atoms distributions to obtain the cumulative distribution of collision times and following the fitting procedure outlined in [20] the collision time is extracted and with it the collisional loss rate. Reaction rates obtained using this model are included in Fig. 2. The calculated rates are comparable to the measured destruction rates and increase linearly with density, ρ. This behavior results because E_{coll} is negligible whereupon Eqn. 7 may be written

$$t \propto -\int_{r_{\mathrm{intial}}}^{r_{\mathrm{final}}} r^2 \mathrm{d}r \propto r_{initial}^3 \tag{8}$$

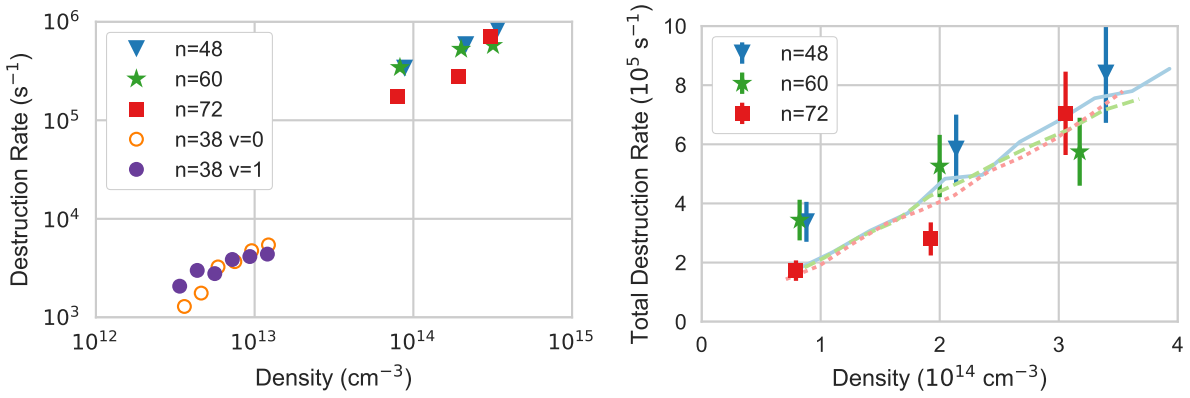

Figure 2. Collisional destruction rates, $\Gamma_{LOSS} = \Gamma_{AI} + \Gamma_L$, as a function of local atom density, ρ. Left: Results obtained in a BEC for the values of n indicated together with earlier results obtained for n=38 vibrational ground-state (ν=0) and first excited-state (ν=1) dimers [21]. Right: Expanded view of high density data with results of model simulations shown with solid, dashed and dotted lines for n of 48, 60 and 72, respectively.

with $r_{\rm final} < r_{\rm initial}$. The reaction rate, which is proportional to $1/t$, thus scales as $1/r^3_{initial}$. Since the nearest-neighbor distance is $\sim \rho^{-1/3}$, the reaction rate will then scale as ρ.

It is instructive to compare the present loss rates with those reported in earlier studies of $n = 38$ strontium dimers to see if the present reaction model based on a close collision between the core ion and a ground-state atom can be applied. In the earlier work cold thermal gases with $\rho \sim 10^{13}$ cm^{-3} and temperatures of ~ 2.2 μK were employed. The measured collisional loss rates again increased linearly with density but were small, $\sim 5 \times 10^3$ s^{-1} at $\rho = 2 \times 10^{13}$ cm^{-3}. These rates, included in Fig. 2, when extrapolated, do not appear to be consistent with the present observations. The earlier results were interpreted in terms of collisions between the Rydberg dimer and neighboring ground-state atoms. This is justified because the mean atom-atom collision velocity, $\langle v \rangle = 3.2 \times 10^{-2}$ m s^{-1}, was such that over the ~ 50 μs duration of the earlier experiments atoms moved ~ 1.5 μm relative to one another which is large compared to the radius of an $n = 38$ dimer, ~ 120 nm. This allowed the collisional loss rate, Γ_{LOSS}, to be written in terms of a collision cross section, σ_{COLL}, as

$$\Gamma_{LOSS} = \rho \sigma_{COLL} \langle v \rangle \tag{9}$$

The data yielded a collision cross section $\sigma_{COLL} \sim 8 \times 10^{-11}$ cm^2 that was significantly smaller than the Langevin cross section for ion-atom collisions, $\sqrt{C_4/E_{coll}} \sim 6 \times 10^{-10}$ cm^2. The geometric cross section of the molecules, $\sim 4\pi n^4$ a.u., i.e., $\sim 5 \times 10^{-10}$ cm^2, is also smaller than the Langevin cross section. Thus for reaction to occur a ground-state atom must enter the Rydberg molecule and pass relatively close to the core ion, i.e., within $\sim 40\%$ of the atomic radius. At such separations the screening of the core ion charge is weak allowing the neutral atom to be attracted to the core ion thereby facilitating reaction. Thus the same reaction model based on a close encounter between the core ion and a ground-state atom can be used to explain the data obtained at both high and low densities, the difference being that at high densities ground state atoms are initially positioned close to the core ion whereas at low densities ground-state atoms must, through relative motions, enter the electron orbit and pass close to the core ion.

The present results show that, even though no p-wave shape resonance is present, strontium Rydberg molecules excited in a BEC are rapidly destroyed, on time scales of a few μs, through

associative ionization and L-changing reactions which places strict limits on the time scales over which studies using such molecules in cold dense atomic gases can be made. Both loss processes, however, require the presence of the Rydberg electron which suggests that for very high n values, where the Rydberg electron probability density near the nucleus becomes very small, the loss rates might begin to decrease. Also it will be interesting to explore the lifetimes of Rydberg molecules created in dense ^{87}Sr samples for which fermion statistics limit the probability for finding two atoms in close proximity.

Research supported by the NSF under Grants Nos. 1205946 and 1600059, by the AFOSR under Grant No. FA9550-12-1-0267, the Robert A. Welch Foundation under Grants No. C-0734 and C-1844, by the FWF (Austria) under Grant No. P23359-N16, and the SFB Nextlite.

References

[1] Greene C H, Dickinson A S and Sadeghpour H R 2000 *Phys. Rev. Lett.* **85**(12) 2458–2461
[2] Bendkowsky V, Butscher B, Nipper J, Shaffer J P, Löw R and Pfau T 2009 *Nature* **458** 1005 ISSN 1476-4687
[3] Li W, Pohl T, Rost J M, Rittenhouse S T *et al.* 2011 *Science* **334** 1110–1114 ISSN 0036-8075
[4] Tallant J, Rittenhouse S T, Booth D, Sadeghpour H R and Shaffer J P 2012 *Phys. Rev. Lett.* **109**(17) 173202
[5] DeSalvo B J, Aman J A, Dunning F B, Killian T C, Sadeghpour H R, Yoshida S and Burgdörfer J 2015 *Phys. Rev. A* **92**(3) 031403
[6] Bellos M A, Carollo R, Banerjee J, Eyler E E, Gould P L and Stwalley W C 2013 *Phys. Rev. Lett.* **111**(5) 053001
[7] Saßmannshausen H, Merkt F and Deiglmayr J 2015 *Phys. Rev. Lett.* **114**(13) 133201
[8] Krupp A T, Gaj A, Balewski J B, Ilzhöfer P, Hofferberth S, Löw R, Pfau T, Kurz M and Schmelcher P 2014 *Phys. Rev. Lett.* **112**(14) 143008
[9] Anderson D A, Miller S A and Raithel G 2014 *Phys. Rev. Lett.* **112**(16) 163201
[10] Booth D, Rittenhouse S T, Yang J, Sadeghpour H R and Shaffer J P 2015 *Science* **348** 99–102 ISSN 0036-8075
[11] Eiles M T and Greene C H 2015 *Phys. Rev. Lett.* **115**(19) 193201
[12] Eiles M T, Lee H, Pérez-Ríos J and Greene C H 2017 *Phys. Rev. A* **95**(5) 052708
[13] Gaj A, Krupp A T, Balewski J B, Löw R, Hofferberth S and Pfau T 2014 *Nat. Comm.* **5** 4546 ISSN 2041-1723
[14] Dunning F B, Killian T C, Yoshida S and Burgdörfer J 2016 *J. Phys. B: At. Mol. Opt. Phys.* **49** 112003
[15] Butscher B, Bendkowsky V, Nipper J, Balewski J B *et al.* 2011 *J. Phys. B: At., Mol. and Opt. Phys.* **44** 184004 ISSN 0953-4075
[16] Camargo F, Schmidt R, Whalen J D, Ding R, Woehl Jr G, Yoshida S, Burgdörfer J, Dunning F B, Sadeghpour H R, Demler E and Killian T C 2017 *ArXiv:1706.03717*
[17] Karpiuk T, Brewczyk M, Rzewski K, Gaj A, Balewski J B, Krupp A T *et al.* 2015 *New Journal of Physics* **17** 053046
[18] Niederprüm T, Thomas O, Eichert T, Lippe C, Pérez-Ríos J, Greene C H and Ott H 2016 *Nat. Comm.* **7** 12820
[19] Wang J, Gacesa M and Côté R 2015 *Phys. Rev. Lett.* **114**(24) 243003
[20] Schlagmüller M, Liebisch T C, Engel F, Kleinbach K S, Böttcher F *et al.* 2016 *Phys. Rev. X* **6**(3) 031020
[21] Camargo F, Whalen J D, Ding R, Sadeghpour H R, Yoshida S, Burgdörfer J, Dunning F B and Killian T C 2016 *Phys. Rev. A* **93**(2) 022702
[22] Stellmer S, Schreck F and Killian T C 2014 *Annual Review of Cold Atoms and Molecules Volume 2* ed Madison K W, Bongs K, Carr L D, Rey A M and Zhai H (Hackensack, NJ: World Publishing Co. Pte. Ltd.) chap 1, pp 1–80 ISBN 978-981-4590-16-7